Quantum chemical SINDO1 study of vanadium pentoxide

Nurbosyn U. Zhanpeisov [1], Thomas Bredow and Karl Jug

Theoretische Chemie, Universität Hannover, Am Kleinen Felde 30, 30167 Hannover, Germany

Received 5 July 1995; accepted 10 February 1996

An improved set of parameters for vanadium in the semiempirical quantum chemical SCF MO method SINDO1 is presented. It is shown that both the geometries and heats of formation of a number of vanadium-containing compounds calculated by this method are in good agreement with available experimental data. Model clusters of increasing size are used for the study of geometric and energetic properties of vanadium pentoxide. Both hydrogen atom and proton adsorption on the (010) surface of vanadium pentoxide and a subsequent formation of different oxygen vacancies have been investigated. Based on these computational results the reactivities of V_2O_5-surface oxygen atoms for adsorption are discussed.

Keywords: vanadium pentoxide; H and H^+ adsorption; oxygen vacancies; quantum chemical study

1. Introduction

Vanadia-based catalysts with vanadium pentoxide as a main component are widely used for various processes such as (i) selective catalytic reduction of nitric oxide by ammonia, (ii) both selective and total oxidation of hydrocarbons and sulfur dioxide, (iii) formation of cathode energy batteries and metal bronzes, etc. [1–3]. Numerous experimental investigations have been reported in the literature dealing with synthesis, characterization and direct study of optical, electronic and magnetic properties of vanadium pentoxide using modern spectroscopic and other experimental techniques [4–7]. On the other hand, only a small number of theoretical investigations have been reported. This is not surprising since the crystal structure of vanadium pentoxide has a rather complicated molecular building block, which may be one of the inherent problems of theoretical modeling and interpretation of experimental data.

For example, Hückel type calculations for small charged fragments (VO_6^{7-} or VO_4^{3-}) simulating vanadium pentoxide have been performed in refs. [8,9]. The results obtained are used for interpretation of X-ray emission spectra. The CNDO CI method was applied to study the electronic structure and optical transitions for V_2O_5 using $VO_n^{(5-2n)}$ clusters with $n = 4, 5, 6$ [10]. These clusters correspond to tetra-, penta- and hexacoordinated vanadium centers in the oxide lattice. It was shown that the fine structure of the optical spectra is connected with the covalent splittings of the vanadium 3d and oxygen 2p atomic levels. Xα methods (both Xα-DV and Xα-SW) were applied to study the electronic structure and to interpret the photoelectron and X-ray spectra of vanadium pentoxide modeled by VO_4^{3-} clusters [11–13].

The adsorption of hydrogen and subsequent removal of OH from the vanadium pentoxide (010) surface has been studied on the ab initio level [14,15]. The process is modeled by small V_2O_9, V_2O_9H and V_2O_8OH model clusters. However, these model clusters do not correctly describe the coordination of the six boundary oxygens and do not take into account the influence of the rest part of the vanadium pentoxide lattice. In contrast to a generally assumed mechanism on the most important role of vanadyl oxygen in catalytic oxidation reactions [16–18], these authors found that the adsorption of hydrogen as H^+ on V_2O_9 and subsequent desorption of an OH group and an oxygen surface vacancy formation turns out to be more favorable on the bridged sites compared to vanadyl oxygen site by energetics. Recent DFT calculations by Hermann et al. [19] on the neutral saturated $V_2O_9H_8$ cluster yield the same qualitative results. This result is in qualitative agreement with a conclusion from semiempirical INDO studies using the same model clusters [20] that it is the bridging oxygen site rather than the vanadyl site which is involved in the process of the selective oxidation of toluene into benzaldehyde on the vanadium pentoxide catalyst. Earlier, the same type of result had been obtained with both IR spectroscopy and a semiempirical INDO method based on crystal orbital formalism using two structural models for vanadium pentoxide [21]. In the first model, a two-dimensional V_2O_5 monolayer was used. Atomic interactions within the sphere of radii 5.5 Å around each atomic center are treated quantum mechanically while the rest is expressed in terms of the conventional electrostatic Madelung approximation. The second model, which corresponds to a $(V_2O_5)_4(H_2O)_2$ one-layer molecular cluster was directly applied for the study of the defect energies associated with three types of oxygen vacancies. Based on these computational results they also concluded that the most stable vacancy corresponds to the

[1] Visiting Scientist. Permanent address: Institute of Catalysis, Prosp. Lavrentieva 5, Novosibirsk 630090, Russia.

removal of a bridged tricoordinated oxygen site rather than dicoordinated bridging and/or vanadyl oxygen sites and this former oxygen is the most relevant one in the oxidation processes involving the catalyst V_2O_5.

In the present work we propose an improved set of parameters for the semiempirical SCF MO method SINDO1 for the consideration of vanadium-containing compounds. In the following we use this method for the study of electronic, energetic and geometric characteristics of vanadium pentoxide. Based on calculations the adsorption of H or H^+ and the formation of different oxygen vacancies on vanadium pentoxide will be discussed.

2. Method of calculation and parametrization

In the following quantum chemical calculations are performed with the semiempirical SCF MO method SINDO1. Its main features are given in refs. [22–25]. The parameters in the SINDO1 method can be divided into two classes: fixed atomic and adjustable atomic and bond parameters [23–25]. The first set of parameters for the vanadium atom, which can be either obtained from experimental data or calculated, are taken from the original version of SINDO1 [24]. As for adjustable atomic and bond parameters, we have systematically studied their influence on calculated values of heats of formation and geometries for some vanadium-containing compounds. It was found that satisfactory agreement with experimental data can be obtained when the atomic orbital exponent ζ_d is set equal to 2.18 instead of 2.31 and only one bond parameter α_{VX} per V–X bond is used instead of α_{VX} and α_{XV} as in ref. [24]. The latter parameters serve to supply the fine adjustment of the V–X bond energy contribution to the total energy contribution. The other adjustable atomic parameters for the vanadium atom are not changed compared to the original version of SINDO1 [24].

Table 1 shows the optimized bond parameters α_{VX} between V and X atoms, where X = H, C, N, O, F, Cl, V. Table 2 compares the results for heats of formation and geometries for a set of vanadium-containing compounds of the previous parametrization [24] and the present parametrization [25] with experimental data [24,26–31]. The agreement between the new calculated data and observed data is quite good. Note in particular the good fit for heats of formation for V_2, VO_2, VF_5, $VOCl_3$. A relatively large error is found in the present version for V–C bond lengths in $C_5H_5V(CO)_4$ and $V(CO)_6$. However, there are no exact experimental data on the heats of formation of these compounds. Moreover, the experimental geometry of the former compound, which was found from three-dimensional X-ray analysis, corresponds to the crystal structure. For compound $NVCl_4$ we found also another minimum which is 2.4 kcal/mol more stable than the former one and has the following bond lengths and bond angles: ClN = 1.705 Å; NV = 1.670 Å; VCl = 2.226 Å; ClNV = 112.9°; NVCl = 105.6°. Perhaps there are two minima, one of which is localized at a ClNV angle about 170° and second one at 113°.

Table 1
Adjusted new set bond parameters α_{VX} for vanadium with X = H, C, N, O, F, Cl, V

Bond type	α_{VX}	Bond type	α_{VX}
V–V	0.473	V–O	0.359
V–H	0.370	V–F	0.185
V–C	1.750	V–Cl	0.170
V–N	0.694		

The molecular bond parameter α_{AB} for A–B interaction is not optimal for the description of bonding situations in solid-state-like structures [32–34]. Therefore α_{VO} was slightly modified in order to reproduce the solid state properties of vanadium pentoxide. This is in accordance with ab initio calculations for adsorption processes on metal oxide surfaces, in which different basis sets were used for the O atoms of the adsorbed molecules and of the surface oxide anion (see, for example, ref. [35]).

3. Cluster models for vanadium pentoxide

The crystal lattice of V_2O_5 monocrystals is characterized by the P_{mmn} space group (No. 59) [21] with unit cell parameters $a = 11.51$ Å, $b = 3.56$ Å, and $c = 4.37$ Å, respectively [36]. It can be described by distorted trigonal bipyramids [7,8,37], orthorhombic [21] or strongly distorted octahedral [20] structures sharing edges and forming infinite double ribbons parallel to the b-axis (fig. 1). These ribbons or chains are linked by pyramid corners forming puckered layers perpendicular to the c-axis (fig. 1). Each vanadium atom is coordinated to five oxygens of the same layer with interatomic distances equal to 1.58, 1.78, 1.88, 1.88 and 2.02 Å [36]. The larger and much weaker V–O bond (bond length equal to 2.79 Å [36]) is formed between a V atom and the nearest vanadyl oxygen atom of the next V_2O_5 layer. So the coordination number of a vanadium bulk atom in vanadium pentoxide is formally equal to 6, even though the V–O bonds have different bond strength.

Quantum chemical cluster calculations are performed with the semiempirical method SINDO1. Vanadium pentoxide was modeled using one- to four-layer clusters (fig. 2) of composition $(V_2O_5)_8H_2O$ (I), $(V_2O_5)_{12}(H_2O)_2$ (II), $(V_2O_5)_{15}H_2O$ (III), $(V_2O_5)_{16}(H_2O)_2$ (IV), $(V_2O_5)_{24}$-H_2O (V), $(V_2O_5)_{24}(H_2O)_3$ (VI), $(V_2O_5)_{30}(H_2O)_2$ (VII), $(V_2O_5)_{32}(H_2O)_2$ (VIII) and $(V_2O_5)_{32}(H_2O)_4$ (IX). The dangling boundary oxygens are saturated by hydrogen atoms forming terminal hydroxyl groups. The positions of these hydrogens are fixed (O–H bond length, 0.96 Å,

Table 2
Heats of formation $\Delta_f H_0^\circ$ (kcal/mol) and geometries (bond length (Å), bond angle (deg)) for some vanadium-containing substrates with previous version [a] and present version [b] of SINDO1

Substrate	$\Delta_f H_0^\circ$			Geometry			
	exp. [a]	calc. [a]	calc. [b]	length/angle	exp. [a]	calc. [a]	calc. [b]
$^3V_2$	187	173.2	186.6	V–V	1.77	1.805	1.765
^5VH	120	121.8	120.4	V–H	1.719	1.768	1.724
^4VO	30.5	33.1	21.4	V–O	1.589	1.628	1.595
$^4VO_2$ [c]	−55.1	–	−55.1	V–O	1.589	–	1.675
				OVO	110	–	110.0
VN	127	131.7	127.1	V–N	1.612	1.820	1.590
$^4VCl_2$ [d]	−48.5	–	−53.1	V–Cl	–	–	2.246
				ClVCl	–	–	112.0
$^2VCl_4$	−125.3	−130.7	−125.8	V–Cl	2.138	2.231	2.211
$^2VF_4$ [e]	−321	–	−306.0	V–F	–	–	1.679
VF_5	−341.0	−363.1	−340.2	$V–F_{eq}$	1.708	1.721	1.672
				$V–F_{ax}$	1.734	1.731	1.668
$VOCl_3$	−165.5	−192.2	−169.5	V–O	1.570	1.586	1.577
				V–Cl	2.142	2.234	2.222
				ClVCl [f]	111.3	108.7	114.5
VOF_3	–	–	−295.0	V–O	1.570	1.595	1.588
				V–F	1.729	1.727	1.675
				FVF [f]	111.2	109.8	114.8
$NVCl_4$	–	–	−103.8	Cl–N	1.597	1.679	1.675
				N–V	1.651	1.634	1.605
				V–Cl	2.138	2.246	2.225
				ClNV	169.7	167.1	167.5
				NVCl	–	–	103.2
$(C_5H_5)V(CO)_4$ [g]	–	–	–	V–Cp	1.93	1.889	1.850
				V–C(O)	1.94	2.14	2.191
				CVCp	119.8	119.0	123.3
$^2V(CO)_6$ [f]	–	–	–	V–C	2.012	2.014	2.091

[a] Experimental (exp.) and previous SINDO1 values from ref. [24].
[b] Present version [25].
[c] Ref. [26].
[d] Ref. [27], heat of formation for 298 K.
[e] Ref. [28], heat of formation for 298 K.
[f] Ref. [29,30].
[g] Ref. [31].

V–O–H bond angle, 140°). In the calculations the other geometry parameters are optimized. It is worth noting that (I), (II), (III), (V) and (VIII) are related to one-layer, (IV) and (VII) to two-layer, (VI) to three-layer and (IX) to four-layer molecular clusters.

At first, two types of geometry optimization were performed for the relatively small $(V_2O_5)_8H_2O$ one-layer cluster. In the first case, full geometry optimization was performed, while in the second case the V–O bond length for all three tricoordinated oxygens (O_{3c}) were set equal to one and the same value and optimized. Thus, in the first case we were able to distinguish between two sets of V_{5c}–O_{3c} bonds, two of which have the same bond length, while the third has a different bond length. It is worth noting that the border oxygens and those oxygens which attached to tetracoordinated vanadium atom (V_{4c}) are also independently optimized. Table 3 shows these optimized geometry characteristics and relative total energies for $(V_2O_5)_8H_2O$, in which all sets of bond lengths and bond angles around the central pentacoordinated vanadium atom (V_{5c}) are presented. The labeling of atoms is in fig. 3. As is clear, the second geometry optimization results in no drastic changes of VO_5 fragment characteristics of $(V_2O_5)_8H_2O$ cluster compared to the first. Moreover, the latter leads only to a little stabilization (7.2 kcal/mol) of the whole cluster compared to the former one. Taking this into account and to save computing time, the second geometry optimization was performed throughout for all other cluster models.

Table 4 shows the optimized geometry characteristics of these molecular clusters simulating vanadium pentoxide together with the experimental bulk values. Only the environment of pentacoordinated V_{5c} for one-layer and of bulk hexacoordinated V_{6c} for multiple-layer clusters together with main lattice parameters are given. As is clear the increase of cluster size for one-layer clusters has practically no influence on the geometry of central pentacoordinated vanadium atom, while transition from one-layer to multiple-layer clusters causes strong changes on the geometry of the vanadium atom environment of interest. Thus, for example, the $O^{(1)}VO^{(2)}$ angle (fig. 3) drastically decreases, while the $O^{(1)}VO^{(3)}$

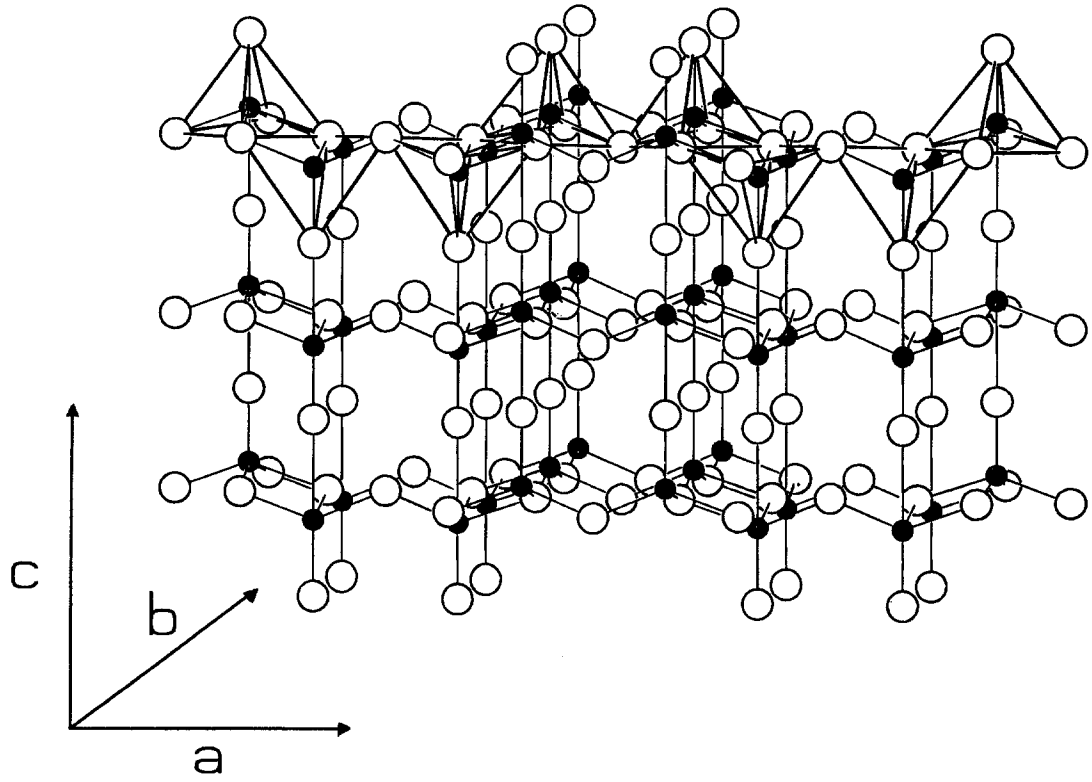

Fig. 1. Crystal structure of vanadium pentoxide simulated by a three-layer cluster $(V_2O_5)_{24}(H_2O)_3$ (• V, ○ O, ○ H).

angle slightly increases when one considers the clusters (I), (IV), (VI) and (IX) (transition from one- to four-layer clusters) or (III) and (VII) (transition from one- to two-layer cluster). The increase in the number of layers also leads to shortening of the lattice parameter c, while the lattice parameter b is practically unchanged and differs only slightly from the experimental reference value. The discrepancy between the theoretical $VO^{(5)}$ value and the corresponding bulk value for the spacing between two layers is not energetically important, because the potential surface is very flat with respect to this coordinate. The distances for the stronger bonds are in good agreement with experiment. The calculated atomic charges for the VO_5 fragment of $(V_2O_5)_{15}H_2O$ and for the VO_6 fragment of $(V_2O_5)_{30}(H_2O)_2$ clusters as representatives of one-layer and multiple-layer clusters are given in table 5 . As expected, vanadium atoms are positively charged and oxygen atoms are negatively charged. The increase in the coordination number of both vanadium and oxygen atoms leads to an increase in the effective charges. The effective charge on tetracoordinated V_{4c} ($q = 1.38$) is less than on the V_{5c} site ($q = 1.42$) for cluster (III) or formally pentacoordinated V_{5c} ($q = 1.43$) for cluster (VII). Bulk vanadyl oxygen is also more negatively charged compared to surface vanadyl oxygen.

Now let us consider the quantum chemical binding energy per unit of panadium pentoxide (E_{Bu}) based on these cluster model calculations, since this energetic property is most important and can be easily compared with the experimental heats of atomization related to the bulk, if the zero-point energy per unit of the lattice is neglected. Recently [32] we observed an increase an increase of E_{Bu} in dependence of a relative average coordination number. We subsequently showed that for stoichiometric ion crystal clusters the dependence of E_{Bu} on the relative average coordination number k has a simple linear relationship [33,38],

$$E_{Bu} = ak + b. \tag{3.1}$$

In our case of vanadium pentoxide, k is defined as the average ratio of all coordination numbers of vanadium atoms in the cluster and the ideal coordination number 6 in the bulk. The linear relationship does not depend on the latter assumption. If coordination number 5 would be assumed due to the weak bond $V\text{–}O^{(5)}$, the a and b values in (3.1) would have to be changed for adjustment to the bulk E_{Bu} value. This implies a change of the α_{VO} value. Since we used clusters saturated with H and OH throughout, E_{Bu} is calculated as

$$E_{Bu} = [E_B((V_2O_5)_n(H_2O)_m) - \tfrac{3}{2}mE_B(H_2O)]/n. \tag{3.2}$$

It should be noted that eq. (3.2) is only an approximation, because in the case of saturation a V–O bond is replaced by an H–O bond.

In fig. 4 the binding energy E_{Bu} is presented in dependence on the relative average coordination number k. We observe a linear increase of E_{Bu} with increasing k. The extrapolated bulk value from SINDO1 is 903.0 kcal/mol for E_{Bu} compared to 909.8 kcal/mol [26] from

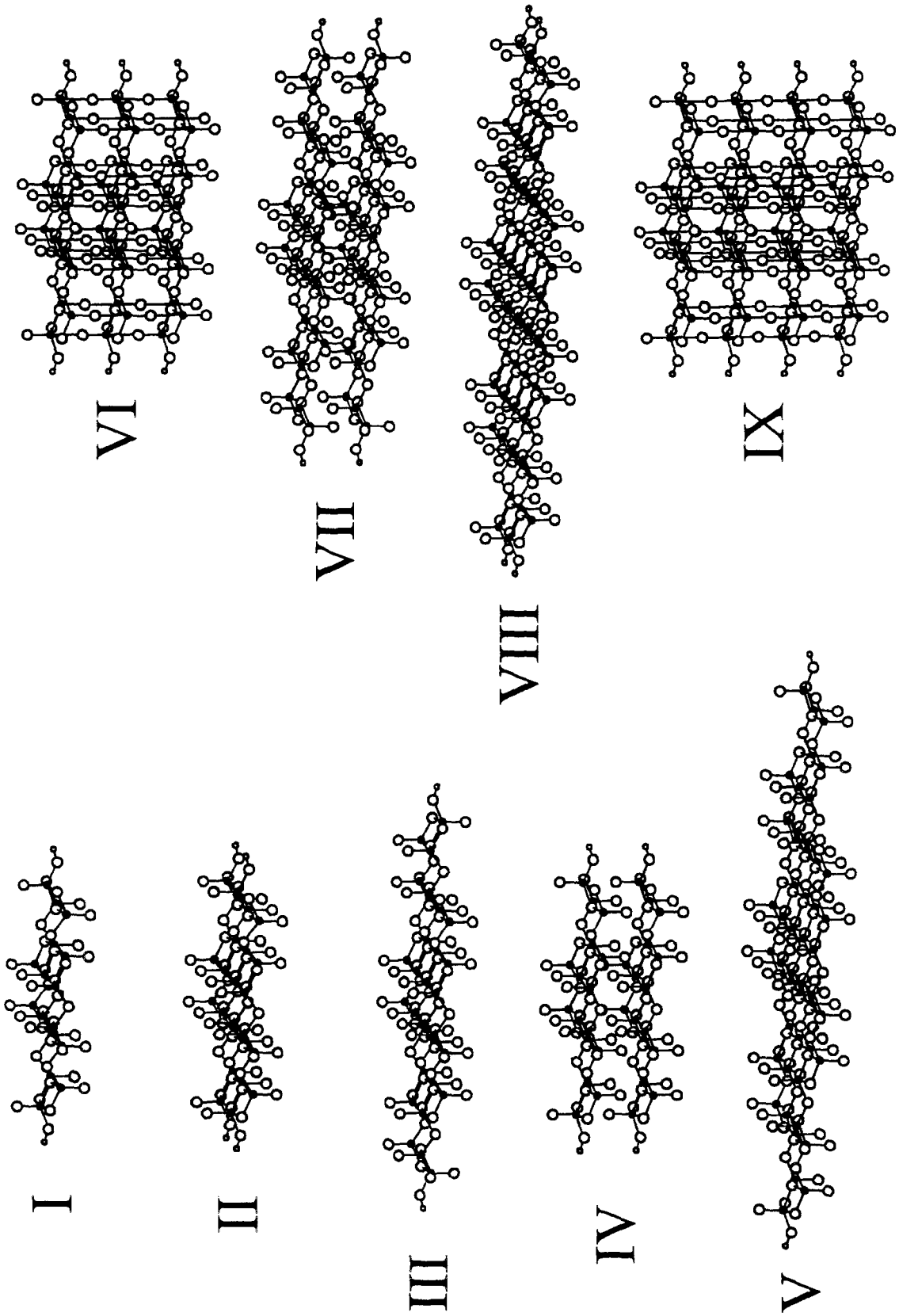

Fig. 2. Shapes of model clusters I–IX specified in text.

Table 3
Geometry (bond length (Å), bond angle (deg)) and relative total energies E_{rel} (kcal/mol) of $(V_2O_5)_8H_2O$ model cluster calculated with SINDO1

Length/angle [a]	Opt.1 [b]	Opt.2 [c]	Exp. [d]
$VO^{(1)}$	1.646	1.646	1.58
$VO^{(2)}$	1.763	1.760	1.78
$VO^{(3)}$	1.823	1.827	1.88
$VO^{(4)}$	1.848	1.827	2.02
$O^{(1)}VO^{(2)}$	124.5	123.8	
$O^{(1)}VO^{(3)}$	101.2	101.2	
$O^{(1)}VO^{(4)}$	113.2	113.2	
E_{rel}	0	7.2	

[a] Labels of atoms from fig. 3.
[b] Full geometry optimization.
[c] Restricted geometry optimization ($VO_{(3)} = VO_{(4)}$).
[d] Bulk structure [36].

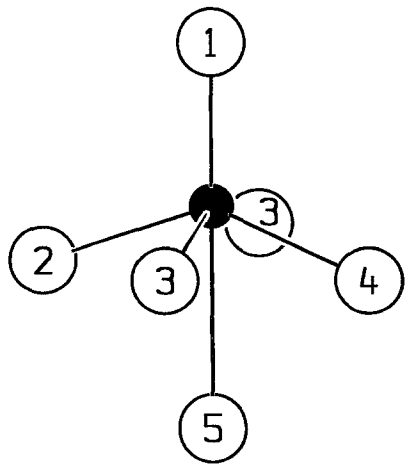

Fig. 3. Labeling of oxygen atoms around a central vanadium atom.

experiment. This comparison is justified, because the zero point energy per unit will not exceed a few kcal/mol. Thus, we conclude that SINDO1 is a suitable method for the consideration of bulk properties of vanadium pentoxide.

4. Oxygen reactivity in vanadium pentoxide

In order to clarify the reactivity of oxygens at different oxygen sites on the (010) surface of vanadium pentoxide, we performed additional calculations modeling (i) the formation of the different types of oxygen vacancies, (ii) adsorption of H or H^+ at the different surface oxygens. In fact, on this surface we have five different oxygen sites (fig. 5): the vanadyl oxygen site A, the oxygen site B bridging two vanadyl groups, the oxygen site C bridging two vanadium atoms, the oxygen site D bridging two vanadyl groups and one vanadium atom, and finally, the oxygen site E bridging one vanadyl group and two vanadium atoms. A first type of calculation can be performed by simply creating a vacancy site on the respective precursor oxygen site in optimized and nonrelaxed crystal structures and a second type by local optimization of the geometry of the considered oxygen site and the adsorbed hydrogen or proton.

Table 6 shows the relative total energies of the cluster (III) with an oxygen vacancy. The calculations have been performed for three different net charges of $q = 0$, $+1$, $+2$ of this cluster. For $q = 0$ a neutral oxygen atom is removed, for $q = +1$ an oxygen anion and for $q = 2$ an oxygen dianion is removed. For each net charge, the total energy of the most stable vacancy structure has been taken as internal reference. As is clear the ordering of stabilities of oxygen vacancies on vanadium pentoxide is O_{3c} (D site) < O_{3c} (E site) < O_{2c} (B site) < O_{2c} (C site) ≈ O_{1c} (A site).

In accordance with refs. [16–18] this order shows that the creation of an oxygen vacancy at the precursor vanadyl oxygen site is energetically more profitable compared to the bridging oxygen sites. This means that the energy necessary to create an oxygen vacancy on the bridging sites is more costly than on vanadyl oxygen site. This is also true if one takes into account the relative concentration of vanadyl sites compared to dicoordi-

Table 4
Geometry characteristics (length (Å), bond angle (deg)) of various vanadium pentoxide clusters calculated with SINDO1 [a]

Length/angle	I	II	III	IV	V	VI	VII	VIII	IX	Exp. [b]
$VO^{(1)}$	1.646	1.645	1.647	1.644	1.647	1.645	1.645	1.647	1.646	1.58
$VO^{(2)}$	1.760	1.762	1.762	1.749	1.763	1.744	1.749	1.763	1.742	1.78
$VO^{(3)}$	1.827	1.827	1.827	1.840	1.827	1.843	1.838	1.828	1.844	1.88
$VO^{(5)}$	–	–	–	2.339	–	2.235	2.377	–	2.227	2.79
$O^{(1)}VO^{(2)}$	123.8	123.6	123.8	116.8	123.7	113.2	116.6	123.4	112.4	
$O^{(1)}VO^{(3)}$	101.2	102.6	101.6	104.5	101.9	104.4	105.4	102.7	104.4	
$O^{(1)}VO^{(4)}$	113.2	114.0	114.5	111.1	114.7	109.2	112.4	115.2	109.2	
a	12.132	12.147	12.109	12.799	12.116	13.104	12.783	12.141	13.150	11.51
b	3.586	3.567	3.580	3.563	3.575	3.571	3.544	3.567	3.572	3.56
c	–	–	–	3.983	–	3.880	4.022	–	3.873	4.37

[a] Roman numbers correspond to different model clusters simulating vanadium pentoxide (see also text).
[b] Bulk structure [36].

Table 5
Atomic charges for VO_5 fragment of the cluster (III) and for VO_6 fragment of the cluster (VII) calculated with SINDO1

Atom	III	VII
$O^{(1)}$	−0.41	−0.45
V	1.42	1.51
$O^{(2)}$	−0.58	−0.57
$O^{(3)}$	−0.69	−0.70
$O^{(3)a}$	−0.73	−0.74
$O^{(4)}$	−0.73	−0.76
$O^{(5)}$	–	−0.56

[a] Oxygen atom attached to a vanadium atom with fewer oxygen neighbors than others.

nated bridging oxygen sites (B and C). In the unit cell the former is two times higher than the latter.

Now let us consider the interaction of H or H^+ with these surface oxygen atoms of vanadium pentoxide simulated by the same cluster (III). Table 7 shows the relative total energies ΔE for hydrogen atoms and protons adsorbed on these surface complexes. The energetically most preferable complex is taken as internal reference in each case. The most important geometry characteristics of these adsorption complexes are also presented. In the calculations two parameters are optimized within the symmetrical restrictions, namely, O–H bond distance and relaxation value ΔR of the oxygen site in the direction of adsorbed particle. The latter is the difference between an optimal position of the oxygen atom in the adsorption complex and in the isolated initial cluster. As can be seen from table 7 the adsorption of both hydrogen atom and proton is energetically more favorable on the vanadyl oxygen site A and on the bridging dicoordinated oxygen site C, because they display comparable reactivity. In both cases the oxygen atom is slightly moved out of the surface by the adsorbed particles. This effect is more pronounced in the case of adsorption on tricoordinated bridging oxygen sites D and E. However, from an energetic point of view they are

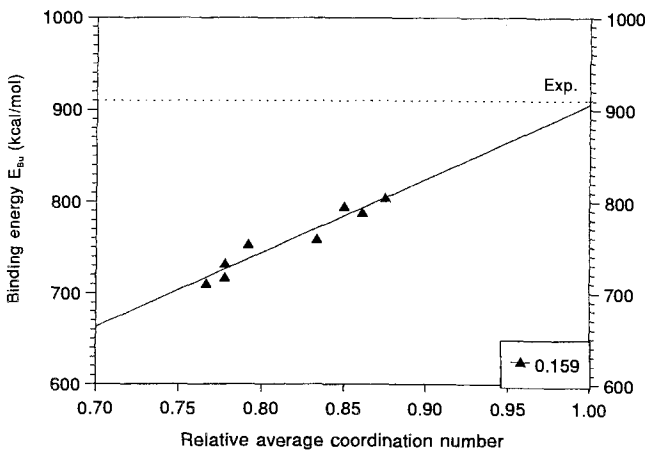

Fig. 4. Binding energy (kcal/mol) per unit E_{Bu} in dependence of relative coordination number k for vanadium pentoxide.

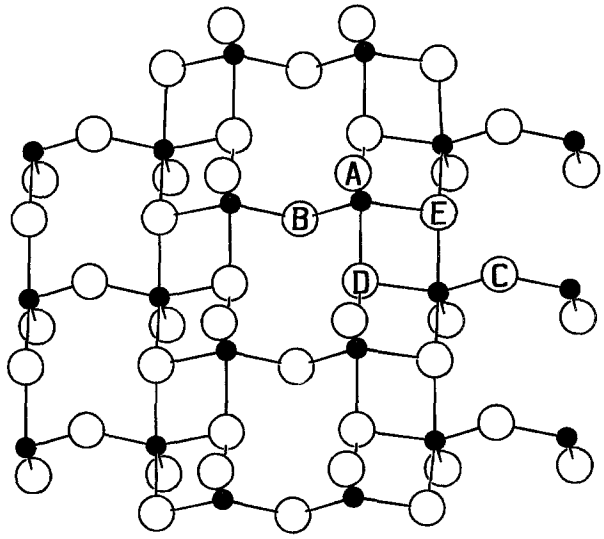

Fig. 5. Labeling of different oxygen sites A–E for the vanadium pentoxide(010) surface.

less profitable. Adsorption on the oxygen site B is less profitable in both cases due to the influence of the two vanadium atoms close by. In this case we found that both H and H^+ are closer to a vanadium atom than to an oxygen atom of interest.

This result is in contrast to other theoretical results in the literature [14,15,19] where hydrogen adsorption on the bridging oxygen site B is found to be energetically preferable compared to the vanadyl oxygen site A. One of the reasons could be that in ref. [14], the V–O bond lengths for all oxygen atoms except the vanadyl oxygen atoms are set equal to one and the same value obtained from averaging the experimental bond distances for the VO_4 fragment. As a result the V–O bond length for the bridging oxygen is longer than the respective experimental value.

Based on our model cluster studies we can conclude that the active site of vanadium pentoxide is probably associated with the terminal V=O groups. Therefore we expect that in catalytic hydrocarbon oxidation reactions in the absence of oxygen molecules, the C–H bond breaking occurs at these centers. However, these hydrogens will be accumulated on the surface of the vanadium pentoxide to form different type of bronze. Water mole-

Table 6
Relative total energies (eV) of the cluster (III) with an oxygen vacancy as calculated with SINDO1 [a]

Vacancy	Site	$q = 0$	$q = +1$	$q = +2$
O_{1c}	A	0	0	0.54
O_{2c}	B	0.41	1.30	0.30
O_{2c}	C	0.40	1.18	0
O_{3c}	D	2.43	2.83	2.30
O_{3c}	E	2.10	1.76	1.90

[a] Positive energy increments indicate destabilization of the defect structure (see also text).

Table 7
Relative total energies E_{rel} (eV) of H and H^+ adsorbed surface complexes, O–H distance (Å), oxygen relaxation ΔR (Å) calculated with SINDO1 [a]

Site	Hydrogen			Proton		
	E_{rel}	OH	ΔR	E_{rel}	OH	ΔR
A	0.24	0.967	0.051	0.11	0.970	0.048
B	8.52	0.984	−0.150	8.30	0.982	−0.150
C	0	0.979	0.206	0	0.975	0.178
D	3.03	1.010	0.610	3.33	1.026	0.356
E	3.57	1.052	0.413	3.65	1.044	0.371

[a] See footnote of table 6.

cules can be directly formed only in the presence of gaseous oxygen, since the formation of the oxygen vacancy centers and their recovery by incoming gaseous oxygens are interrelated processes.

5. Conclusion

Model clusters of varying surface and layer size were used for the study of the formation of O vacancies and H and H^+ adsorption on the $V_2O_5(010)$ surface. It was found that symmetry restricted, bulk-like optimization of the cluster structure and local relaxation are important for the description of these processes. Our procedure emphasizes the use of neutral, saturated stoichiometric clusters, where all cluster atoms in the adsorption region have the proper environment. This reduces artefacts from the cluster model.

Acknowledgement

This work was supported by Deutsche Forschungsgemeinschaft and the Commission of the European Communities. The calculations were performed on a HP9000/735 workstation cluster and the Siemens S400/40 at Universität Hannover. We thank Professor K. Hermann for a preprint of his recent results on vanadium pentoxide.

References

[1] A. Andersson, in: *Adsorption and Catalysis on Oxide Surface*, eds. M. Che and G.C. Bond (Elsevier, Amsterdam, 1985).
[2] M.S. Whittingham, J Electrochem. Soc. Electrochem. Sci. Technol. 123 (1976) 315.
[3] K. Mori, A. Miyamoto and Y. Murakami, J. Phys. Chem. 94 (1990) 5029.
[4] J. Le Bars, J.C. Vedrine, A. Auroux, B. Pommier and G.M. Pajonk, J. Phys. Chem. 96 (1992) 2217.
[5] F.D. Hardcastle and I.E. Wachs, J. Phys. Chem. 95 (1991) 5031.
[6] J.C. Parker, D.J. Lam, Y.-N. Xu and W.Y. Ching, Phys. Rev. B 42 (1990) 5289.
[7] J.M. Cocciantelli, P. Gravereau, J.P. Doumerc, M. Pouchard and P. Hagenmuller, J. Solid State Chem. 93 (1991) 497.
[8] N.I. Lasukova, V.A. Gubanov and R.N. Pletnev, Int. J. Quant. Chem. 9 (1975) 691.
[9] P.E. Best, J. Chem. Phys. 44 (1966) 3248.
[10] N.I. Lasukova, V.A. Gubanov and V.G. Mokerov, Int. J. Quant. Chem. 12 (1977) 915.
[11] A.V. Kondratenko, E.S. Fomin, V.I. Nemanova, S.F. Rusankin, G.M. Zhidomirov and L.N. Masalov, Zh. Strukt. Khim. 30 (1989) 92.
[12] N.V. Dobrodei, A.V. Kondratenko and G.L. Gutsev, Zh. Fiz. Khim. 63 (1989) 120.
[13] S.G. Gagarin and Yu.V. Plekhanov, Kinet. Katal. 25 (1984) 37.
[14] M. Witko and K. Hermann, J. Mol. Catal. 81 (1993) 279.
[15] M. Witko, K. Hermann and R. Tokarz, J. Electron Spectrosc. Relat. Phenom. 69 (1994) 89.
[16] H.H. Kung, *Transition Metal Oxides: Surface Chemistry and Catalysis*, Studies in Surface Science and Catalysis, Vol. 45 (Elsevier, Amsterdam, 1989).
[17] A. Miyamoto, Y. Yamazaki, M. Inomata and Y. Murakami, J. Phys. Chem. 85 (1981) 2366.
[18] J. van Ommen and J. Ross, Appl. Catal. 25 (1986) 239.
[19] K. Hermann, A. Michalak and M. Witko, Catal. Today, submitted.
[20] M. Witko, J. Haber and R. Tokarz, J. Mol. Catal. 82 (1993) 457.
[21] R. Ramirez, B. Casal, C. Utrera and E. Ruiz-Hitzky, J. Phys. Chem. 94 (1990) 8960.
[22] D.N. Nanda and K. Jug, Theor. Chim. Acta 57 (1980) 95.
[23] K. Jug, R. Iffert and J. Schulz, Int. J. Quantum Chem. 32 (1987) 265.
[24] J. Li, P. Correa de Mello and K. Jug, J. Comput. Chem. 13 (1992) 85.
[25] K. Jug and T. Bredow, in: *Methods and Techniques in Computational Chemistry, METECC-95*, eds. E. Clementi and G. Corongiu (STEF, Cagliari, 1995) p. 89.
[26] M.W. Chase Jr., C.A. Davies, J.R. Downey Jr., D.J. Frurip, R.A. McDonald and A.N. Syverud, *JANAF Thermochemical Tables*, 3rd Ed., Part II, J. Phys. Chem. Ref. Data 14 (1985) Suppl. 1.
[27] I. Barin, *Thermochemical Data of Pure Substances*, Part II, 2nd Ed. (VCH, 1993).
[28] M.Kh. Karapet'yants and M.L. Karapet'yants, *Handbook of Thermodynamic Constants of Inorganic and Organic Compounds* (Ann Arbor, 1970).
[29] V. Perschina, W.-D. Sepp, T. Bastug, B. Fricke and G.V. Ionova, J. Chem. Phys. 97 (1992) 1123.
[30] K.D. Dobbs and W.J. Hehre, J. Comput. Chem. 8 (1987) 861.
[31] J. Li and K. Jug, J. Comput. Chem. 13 (1992) 93.
[32] K. Jug, G. Geudtner and T. Bredow, J. Mol. Catal. 82 (1993) 171.
[33] T. Bredow and K. Jug, Chem. Phys. Lett. 223 (1994) 89.
[34] T. Bredow and K. Jug, Surf. Sci. 327 (1995) 398.
[34] M. Pöhlchen and V. Staemmler, J. Chem. Phys. 97 (1992) 2583.
[35] H.G. Bachman, F.R. Ahmed and W.H. Barnes, Z. Kristallogr. Kristallgeom. Kristallphys. Kristallchem. 115 (1961) 110.
[36] R.J. Gillespie, *Molecular Geometry* (London, 1972).
[37] K. Jug and G. Geudtner, Chem. Phys. Lett. 208 (1993) 537.